Sympathetic cooling of positrons to cryogenic temperatures for antihydrogen production

C.J. Baker[1], W. Bertsche[2,3], A. Capra[4], C.L. Cesar[5], M. Charlton[1], A. Cridland Mathad[1], S. Eriksson[1], A. Evans[6], N. Evetts[7], S. Fabbri[2], J. Fajans[8], T. Friesen[6], M.C. Fujiwara[4], P. Grandemange[4], P. Granum[9], J.S. Hangst[9], M.E. Hayden[10], D. Hodgkinson[2], C.A. Isaac[1], M.A. Johnson[2], J.M. Jones[1], S.A. Jones[9], S. Jonsell[11], L. Kurchaninov[4], N. Madsen[1], D. Maxwell[1], J.T.K. McKenna[9], S. Menary[12], T. Momose[7], P. Mullan[1], K. Olchanski[4], A. Olin[4] , J. Peszka[1], A. Powell[6], P. Pusa[11], C.Ø. Rasmussen[14], F. Robicheaux[15], R.L. Sacramento[5], M. Sameed[2], E. Sarid[16], D.M. Silveira[5], G. Stutter[9], C. So[6], T.D. Tharp[17], R.I. Thompson[6], D.P. van der Werf[1] and J.S. Wurtele[8] (The ALPHA Collaboration)

[1] Department of Physics, College of Science, Swansea University, Swansea SA2 8PP, UK.
[2] School of Physics and Astronomy, University of Manchester, Manchester M12 9PL, UK.
[3] Cockcroft Institute, Sci-Tech Daresbury, Warrington WA4 4AD, UK.
[4] TRIUMF, 4004 Wesbrook Mall, Vancouver, BC, Canada V6T 2A3.
[5] Instituto de Fisica, Universidade Federal do Rio de Janeiro, Rio de Janeiro 21941-972, Brazil.
[6] Department of Physics and Astronomy, University of Calgary, Calgary AB, Canada T2N 1N4.
[7] Department of Physics and Astronomy, University of British Columbia, Vancouver BC, Canada V6T 1Z1.
[8] Department of Physics, University of California at Berkeley, Berkeley, CA 94720-7300, USA.
[9] Department of Physics and Astronomy, Aarhus University, DK-8000 Aarhus C, Denmark.
[10] Department of Physics, Simon Fraser University, Burnaby BC, Canada V5A 1S6.
[11] Department of Physics, Stockholm University, SE-10691, Stockholm, Sweden.
[12] Department of Physics and Astronomy, York University, Toronto, ON M3J 1P3, Canada.
[13] Department of Physics, University of Liverpool, Liverpool L69 7ZE, UK.
[14] Experimental Physics Department, CERN, Geneva 1211, Switzerland.
[15] Department of Physics and Astronomy, Purdue University, West Lafayette, Indiana 47907, USA.
[16] Soreq NRC, Yavne, 81800, Israel, and Department of Physics, Ben Gurion University, Beer Sheva 8410501, Israel.
[17] Physics Department, Marquette University, P.O. Box 1881, Milwaukee, WI 53201-1881, USA.

Abstract:

The positron, the antiparticle of the electron, predicted by Dirac in 1931 and discovered by Anderson in 1933, plays a key role in many scientific and everyday endeavours. Notably, the positron is a constituent of antihydrogen, the only long-lived neutral antimatter bound state that can currently be synthesised at low energy, presenting a prominent system for testing fundamental symmetries with high precision. Here, we report on the use of laser cooled Be^+ ions to sympathetically cool a large and dense plasma of positrons to directly measured temperatures below 7 K in a Penning trap for antihydrogen synthesis. This will likely herald a significant increase in the amount of antihydrogen available for experimentation, thus facilitating further improvements in studies of fundamental symmetries.

The positron (e^+) plays a unique role in physics. As the most readily available antiparticle, it had a significant role in the development of relativistic quantum mechanics. Its discovery[1] confirmed the landmark predictions made by Dirac[2]. Its availability from radioactive sources meant that it quickly entered the laboratory, where tools such as positron annihilation spectroscopy are used for studies of materials and defects[3,4]. Positrons also play a key role in medical physics, *e.g.,* positron emission tomography can be used to study biological processes *in vivo*[5]. A positron can form

positronium, a short-lived hydrogen-like bound state with an electron, with annihilation limiting the lifetime[6]. This system is a unique, purely leptonic bound state that can be used for tests of fundamental symmetries[7] and is also vital in the study of materials. The key motivation for the study presented here is that positrons and antiprotons can form antihydrogen, either via charge exchange from positronium or via a three-body reaction[8,9,10]. Antihydrogen, which does not appear to occur naturally, is a powerful tool for studying fundamental physics[11]. As an example, we recently found that the 1S-2S transition energy in antihydrogen agrees with that in hydrogen to a level of 2×10^{-12}, the most precise and accurate comparison of hydrogen and antihydrogen to date[12].

A cold, non-neutral plasma of positrons is a crucial ingredient in the only successfully demonstrated method for producing trappable antihydrogen. Synthesis occurs by merging a cold (<20 K) cloud of positrons with a cold cloud of antiprotons[13]. For merging, both species are confined in a cryogenic (~7K) Penning-Malmberg trap, where radial confinement is secured by an axial magnetic field, and axial electric fields are used to confine and manipulate the charged particles along the length of the trap (Figure 1). Experimental and theoretical evidence[13,14] suggests that in the parameter range of current experiments, as opposed to previous ones[15], antiprotons tend to thermally equilibrate with the positrons before antihydrogen is formed during this merging. A consequence is that the temperature of the nascent antihydrogen will be that of the positron plasma. Since, typically, only the tail of the thermal distribution of the formed antihydrogen has low enough energy to be trapped ($\lesssim$0.5 K), achieving a lower positron temperature becomes the cornerstone of improving antihydrogen synthesis and trapping. Here, we report on the use of laser cooled Be^+ ions to sympathetically cool a positron plasma to cryogenic temperatures (~7 K) below those achievable by cyclotron cooling in our trap (~17 K). The resulting positron density and number are comparable to those used for antihydrogen synthesis, and our result thus paves the way for a significant increase in the number of trappable antihydrogen atoms.

Be^+ is the lowest mass ion that is laser-coolable from the ground state, and is therefore widely used for sympathetic cooling (e.g. Refs. 16 and 17). Experiments in 2002 demonstrated sympathetic cooling of a small quantity of positrons ($\sim5\times10^3$) by laser cooled Be^+ ions in a 6 T Penning trap[18] in which the ratio of ions to positrons was 1000:1. For antihydrogen formation and capture in our apparatus, millions of positrons and lower magnetic fields (~1 T) are needed, and antiproton capture by Be^+ ions needs to be minimised, such that a realistic Be^+/e^+ ratio has been estimated[19] to be 1:10. Additionally, the geometry and cryogenic nature of the antihydrogen trap require that a Be^+ ion source cannot be placed closer than about 1.2 m from the trap centre, and that laser access is limited to be essentially on-axis and in one dimension (Figure 1). These constraints currently also limit our solid angle for observing laser-induced fluorescence from trapped ions to be $\sim10^{-6}$ Sr.

Figure 1 shows the layout of the experiment. The Be^+ ions are produced by ablation of Be metal using a 355nm, pulsed (6.3 ns) laser having ~75 μJ per pulse (fluence ~3 J cm^{-2})[20]. The resulting pulse of Be^+ ions is dynamically captured in the left part of the trap system (Figure 1) by using a blocking potential around the centre of the trap and rapidly switching the potential on the first (left-most) electrode. Subsequently, the ions are moved to the axial central region, where there is optimal physical overlap with the 313nm cooling laser. The system for laser cooling is a Toptica TA-FHG pro, frequency locked to a HighFinesse WS8-2 wavemeter. The laser beam is transported through air from a nearby laboratory and injected into the apparatus along a path that is at 2.3˚ to the central axis. Typically, 6 mW is injected. The beam radius (waist) is about 1.2 mm at the location of the ions. Fluorescence from the ions can be observed along a similar path that is azimuthally rotated by 180˚ with respect to the laser path (Figure 1). Be^+ is laser cooled using a laser beam, red detuned from the $2s\ ^2S_{1/2}$ (m_J=1/2, m_I=3/2) – $2p\ ^2P_{3/2}$ (m_J=3/2, m_I=3/2) transition. We rely on off-resonant optical pumping to transfer population into the lower level. The magnetic field in the central region is ~1 T [21]. Positrons are transferred ballistically from a positron accumulator[22] through a magnetic beamline and dynamically trapped in the positron preparation region (Figure 1). After selecting the number of positrons[23], we merge them with the Be^+ ions and the mixture is subsequently compressed using the rotating wall technique (RW)[24], similar to the procedures we have developed for antiproton/electron mixtures[25]. Compression occurs in the positron preparation section, where an azimuthally split electrode is located. For improved compression, the axial B-field is first increased to 3T, using a short solenoid (Figure 1). The mixture is subsequently moved to the central region where the Be^+ can be laser-cooled. Following an experiment, the mixture can be ejected onto a Microchannel Plate/Phosphor (MCP/Phosphor) imaging detector that can also be used as a Faraday Cup. This allows measurement of the radial distribution of the plasmas[26], their axial temperature[27] or their total charge. The axial temperature is extracted by assuming that the cloud is in thermal equilibrium such that the initially released particles originate from the exponential tail of a Boltzmann distribution[27,28]. This also works when the plasma is a mixture of Be^+ and e^+, since the positron-induced signal on the MCP is more than an order of magnitude larger than that of the Be^+, and the Be^+ strike the MCP later due to their larger mass. The axial temperature diagnostic suffers from systematic effects that include plasma cooling as the positron plasma expands in the process of being released, possible radial variation in the length and temperature of the plasma, and systematic errors in fitting the history of the released positrons to the theoretically expected curve. As we are not concerned with absolute comparisons here, we ensure relative consistency by always using the same potential well manipulations for the measurements. The errors on the positron temperatures quoted here are thus based on statistical variations only. The systematic effects may be a large as 50% on the absolute temperature determination[27,28,29].

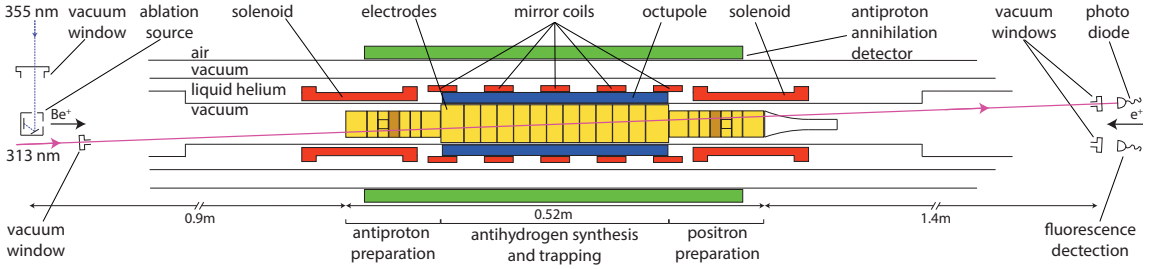

Figure 1 ALPHA trap setup with Be^+ source and cooling laser. The main solenoid supplying a 1T axial field throughout the center is not shown. The cylindrical electrodes (yellow/orange) can be individually charged to provide the axial electric fields for confinement. The central part is to scale. The short solenoids on either end can increase the axial field to 3T in those regions. The positron source and MCP/Phosphor assembly are to the right of the figure but not shown.

In a first set of experiments we prepared a sample of 2.6×10^6 positrons with a radius (in 1T) of 0.54 mm, representative of samples used in our antihydrogen experiments. This sample was merged with 3.8×10^5 Be^+. The Be^+/e^+ mixture was held in the central region in a single-electrode well having an on-axis depth of 70 V. In order to efficiently cool the whole population of Be^+, the laser was initially detuned 104Γ below the cooling transition ($\Gamma = 2\pi \times 19.6$ MHz is the natural linewidth of the transition), and then scanned in 40 s to a final detuning that was varied. The frequency scan time was optimized experimentally to obtain the lowest e^+ temperatures. Figure 2 shows the temperature of the e^+ plasma measured as a function of the final detuning. Between -7Γ and -2Γ, the e^+ temperature reaches a minimum of 6.6±0.5 K, which is a factor ~2.6 below that reported (using an identical temperature diagnostic) for e^+ in synthesis of antihydrogen. For comparison, a Doppler dominated width (HWHM) of 7Γ=140 MHz (the detuning for onset of the temperature minima) would correspond to a Be^+ temperature of 1.5 K.

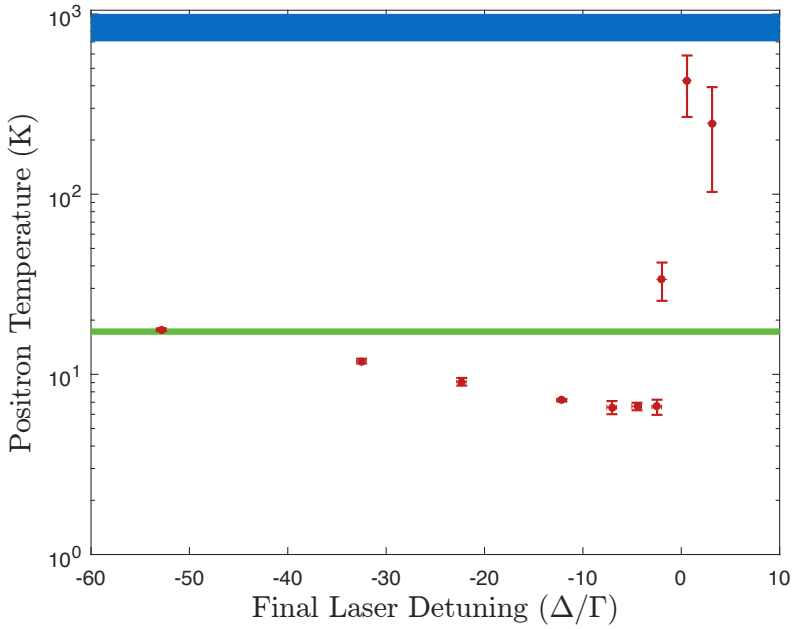

Figure 2 Axial e^+ temperature in a mixed Be^+/e^+ plasma measured as a function of the final detuning of the Be^+ cooling laser. The mixed plasma consisted of 2.6×10^6 e^+, with an initial radius and density of 0.64 mm and $3 \times 10^8 cm^{-3}$ respectively, and $3.8 \pm 0.1 \times 10^5$ Be^+ ions. The laser frequency was swept from an initial detuning of -104 Γ to the final laser detuning in approximately 40 s. The error bars give the standard error of multiple measurements at each setting. The green line shows the e^+ temperature in the absence of any Be^+ ions (17.3±0.5K), and the blue line shows the e^+ temperature when the laser is blocked and the Be^+ ions are not laser-cooled. The shading around these lines indicates the standard error.

The measured minimum e^+ temperature is lower with laser cooled Be^+ present than it is in the absence of either Be^+ or the cooling laser, and the temperature depends on the laser detuning. Thus, Figure 2 clearly shows a sympathetic cooling effect. However, the flat minimum, and the fact that the e^+ temperature is higher than the expected ion temperature for these detunings, indicate that the sympathetic cooling saturates. We cannot exclude that we have reached the lower limit of our temperature diagnostic, but, as we discuss below, centrifugal separation of the two species at these low temperatures likely leads to the observed saturation. The temperatures extracted from those independent measurements are in agreement with those measured here. In addition, the temperature of the mixed plasma without laser cooling is significantly above those typical for e^+ in our apparatus. We believe that the higher than expected temperatures can be attributed to increased heating due to the presence of Be^+. In equilibrium, a strongly coupled, non-neutral plasma rotates rigidly around the axis of the trap with a constant frequency[30]. In a mixed species, non-neutral plasma the species centrifugally separate, with the more massive species accumulating at larger radius[31]. Ion plasmas are, due to their larger mass and lower axial bounce frequencies, more susceptible to field inhomogeneities and expand faster than similar lepton plasmas, the expansion being accompanied by heating [c.f. Ref. 32]. In a mixed plasma, friction between the species drives the accompanying e^+ expansion. We measured the different expansion rates in independent tests (see supplementary material) and found that both Be^+-only and mixed samples expand radially almost two orders of magnitude faster than e^+-only samples in our parameter range.

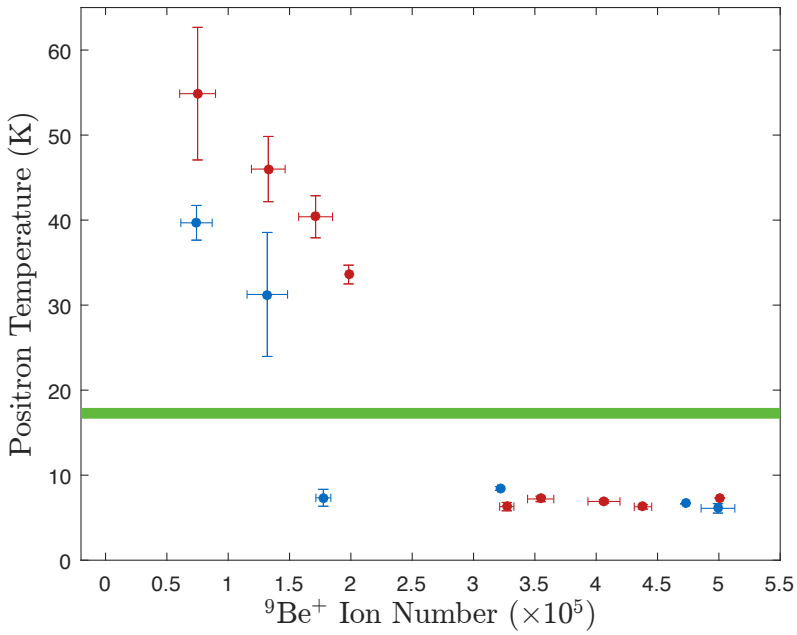

Figure 3 Positron temperature as a function of the number of Be^+ ions used for sympathetic cooling. The ion number has been binned with the horizontal error bars representing the standard deviation of the mean ion number within each bin. The vertical error bars correspond to the standard error on the mean temperature within each bin. The ion number was varied by changing the number of ablation pulses used for loading, and also by splitting the ion plasma using axial potential manipulations. We used 1.4x10^6 positrons (blue points) and 2.6x10^6 positrons (red points) with initial densities of 1x10^8 cm^{-3} and 3x10^8 cm^{-3} respectively. The cooling laser frequency was swept from an initial detuning of -129 Γ to a final detuning of -7 Γ in approximately 40 s for sympathetic cooling of the positrons. The positron temperature for 2.6x10^6 positrons with no ions present (green line) is shown for comparison. The shading around this line indicates the standard error. Note that the positron only temperature for 1.4x10^6 positrons is consistent with this temperature.

As positrons are cooled through collisions with laser-cooled Be^+ ions, increasing the Be^+ to e^+ number ratio could improve sympathetic cooling. To investigate this, we used a fixed final detuning of -7Γ while varying the Be^+ number over a large range, at fixed positron number. Figure 3 shows the final e^+ temperature as a function of the number of Be^+ ions for two different e^+ numbers. What we observe is that in both cases, when the Be^+ number is above a threshold the sympathetic cooling is efficient, yielding a low e^+ temperature that is independent of Be^+ number and consistent with the lowest in Figure 2. The threshold is roughly consistent with a Be^+ to e^+ number ratio of 1:10. When the Be^+ number is too low we measure e^+ temperatures above those observed without ions. The threshold behavior is consistent with the simulations in Ref. 19, where it was determined that strong centrifugal separation at low temperatures caused diminishing returns of further ion number increases; additional ions end up at higher radii and do not contribute to cooling the e^+. The higher than expected temperatures observed with too few Be^+ indicate, as discussed previously, additional heating in the presence of ions.

To investigate the Be^+ radial distribution and thus the centrifugal separation, we first eject the e^+ by lowering the confining potential in the direction opposite to the MCP for ~100 ns, short enough to prevent Be^+ ions from escaping the trap. This is followed almost immediately (~5 μs) by the ejection of the Be^+ towards the MCP for imaging. The delay is minimized to prevent the collapse of the hollow Be^+ distribution[33]. We remove the e^+ first because the e^+ signal overwhelms that of the Be^+ on the MCP. For these measurements we use $2x10^5$ Be^+ and $1.2x10^5$ e^+. Fewer particles were used in this study to ensure that we could correctly image the entire radial extent of the plasma on the MCP after laser cooling. Figure 4 shows MCP images and extracted radial distributions of the Be^+ plasmas ejected in this way for three different final laser detunings. We fitted the measured radial distributions to distributions extracted from self-consistent e^+/Be^+ thermal equilibrium calculations using the N2DEC code from Ref. 33. We find, for the coldest plasma, a temperature of 6.2±0.6 K (Figure 4a), in good agreement with the measured longitudinal e^+ temperature of 7.1±0.5 K. We thus conclude that we have sympathetically cooled the e^+ plasmas in three dimensions to cryogenic temperatures. We also observe, as expected[31,19] , that the amount of separation of the two species increases as the temperature drops, thus reducing the inter-species interactions. While the positron numbers were lower in this part of the experiment, the good agreement with the equilibrium calculations means that centrifugal separation is likely also a key factor in causing the cooling saturation shown in Figure 2.

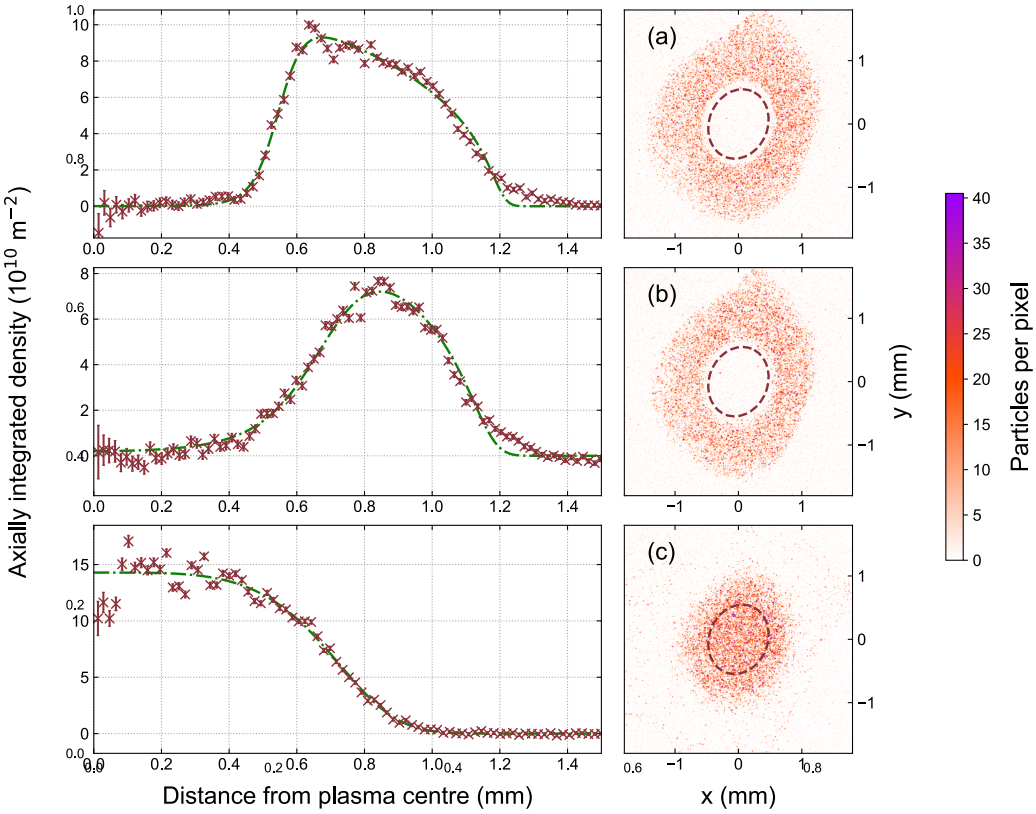

Figure 4 Be⁺ density profiles from originally mixed samples of Be⁺ and e⁺ with 2x10⁵ Be⁺ and 1.2x10⁵ e⁺. The images (right) show Be⁺ ejected to the MCP/Phosphor imaging assembly 5 μs after the ejection of e⁺ in the opposite direction immediately following the laser-cooling of the Be⁺. (a) Laser detuning -20 Γ (b) Detuning -36 Γ (c) Detuning -128 Γ. The measured axial temperatures were (a) 7.1±0.5 K, (b) 10.1 ± 0.2K and (c) 370±100K respectively. To the left of each image is a plot of the extracted axially integrated radial density profile, over-laid with the best fit distribution from calculations assuming thermal equilibrium at the temperatures stated. The fit results were (a) 6.2±0.6K, (b) 19±2K and (c) 253±54K. The corresponding e⁺ densities were (a,b) 6.2±0.1x10⁷ cm⁻³ and (c) 1.2±0.2x10⁸ cm⁻³. The calculations were done using the N2DEC code in Ref. [33] where thermal equilibrium of the two species is assumed. Note that due to the distortion in the imaging, the plasma image is elliptical; the extraction of the radial profile took this into account. Additionally, at higher radii (>1.25mm) the images are distorted by stray electric fields near the MCP as well as physical aperture effects.

Our current fluorescence detection capability is limited to Be^+ temperatures below ~500 mK and cannot be used to determine the temperature of Be^+/e^+ mixtures (see methods). From fluorescence detection we find a typical longitudinal temperature of 200 mK for 10^6 laser-cooled Be^+ ions in our system. This is well below the lowest temperature of our sympathetically cooled e^+. To look for additional heating that may explain this, we examined the e^+ temperature evolution in the mixture with or without sustained laser-cooling. The measurements are shown in Figure 5, where we find that the heating rate is initially 25 K/s for the coldest sympathetically cooled e+. Such temperatures can be maintained for over 20 seconds when laser-cooling remains active, which is much longer that the typically 1 second used for antihydrogen formation in our experiment. In contrast, e^+ prepared alone heat from an initial temperature of ~18K at a rate below 1.5 K/s. The measured mixed plasma heating rate is similar to the rate used in simulations that achieved a low temperature limit of ~5 K[19], in good agreement with the limits observed experimentally. The e^+ temperature increase observed after prolonged sympathetic cooling (Figure 5) is likely due to radial expansion eventually reducing the Be^+ overlap with the cooling laser.

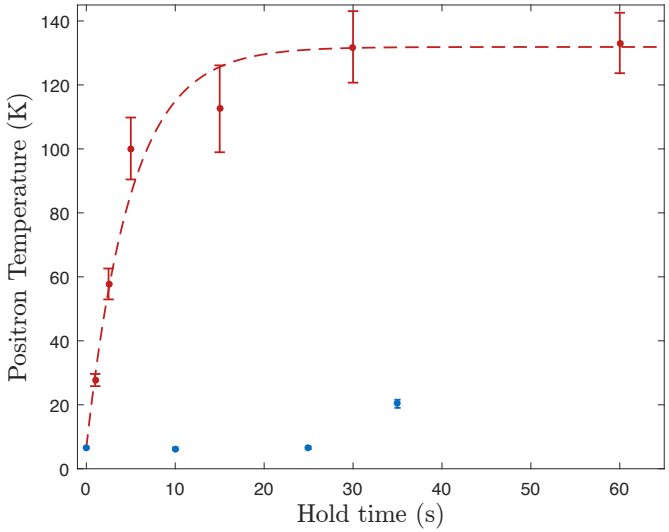

Figure 5 Evolution of the e^+ temperature following the laser cooling frequency sweep for 1.4×10^6 e^+ and $4.7 \pm 0.1 \times 10^5$ Be^+ ions. Turning the cooling laser off (red points) results in the e^+ heating at a rate of approximately 25 K s^{-1}, before their temperature saturates at around 125 K. If, however, the cooling laser is kept on at a fixed detuning of -7 Γ, the final detuning in the frequency sweep, the e^+ can be kept at 6.7 ± 0.3 K for over 20 s (blue points).

We conclude that the observed low temperature limit for sympathetically cooled e^+ is given by the combination of additional heating caused by the presence of Be^+ and the reduced sympathetic cooling as the species centrifugally separate at low temperatures. As discussed previously this heating is likely caused by the Be^+ plasmas rapid expansion, and may, in part be overcome by, *e.g.*, working in higher magnetic fields (like in Ref. 18), or by using shorter potential wells. Higher fields would reduce the depth of the antihydrogen trap, but are only available in the positron and antiproton preparation sections of our trap, where laser-access is foreseen but not currently available. Shorter potential wells can also (currently) only be achieved in the side sections.

Finally, we address the question of the method's compatibility with the inhomogeneous magnetic field of the antihydrogen atom trap. To remain compatible the plasmas must be kept radially small at all times to avoid adverse effects from the transverse octupole magnetic fields of the atom trap[34,35]. To investigate this, we sympathetically cooled 10^5 e^+ with a radial extent of 0.6 mm using 10^5 Be^+ to a temperature of 6.8±0.5 K in the magnetic field used for trapping antihydrogen, thereby demonstrating the feasibility. Unfortunately, the setup currently does not allow laser-cooling while applying the RW compression. We were therefore unable to perform this test on larger e^+ samples, as their radii were too large to avoid the detrimental effects of the non-uniform magnetic fields. Modification of the apparatus to allow laser-cooling during RW and several other improvements are under way to make the system fully compatible with antihydrogen accumulation once antiprotons return to the Antiproton Decelerator at CERN in 2021.

In conclusion, we have demonstrated, by direct measurement of e^+ temperatures and Be^+ radial density distributions, sympathetic cooling of plasmas of millions of e^+ to temperatures below 7 K in three dimensions using laser cooled Be^+ ions. The density and size of the e^+ plasmas as well as the magnetic fields used are commensurate with those used for antihydrogen synthesis and trapping. Efficient sympathetic cooling was also demonstrated in the inhomogeneous fields used to confine antihydrogen. The lowest temperatures are

almost a factor of three lower than the lowest currently used for antihydrogen formation, leading us to expect an improvement in the amount of trapped antihydrogen per mixing attempt of up to a factor of five, thus paving the way for faster and more precise measurements on antihydrogen.

Acknowledgements This work was supported by: CNPq, FAPERJ, RENAFAE (Brazil); NSERC, NRC/TRIUMF, EHPDS/EHDRS, FQRNT (Canada); FNU (NICE Centre), Carlsberg Foundation (Denmark); ISF (Israel); STFC, EPSRC (UK); DOE, NSF (USA); and VR (Sweden).

Author Contributions This experiment was based on data collected using the ALPHA-2 antihydrogen trapping apparatus, The ALPHA-2 apparatus was designed and constructed by the ALPHA Collaboration using methods developed by the entire collaboration. All authors contributed to this work as members of the ALPHA antihydrogen collaboration. The experiment was first suggested by NM. The Beryllium setup was designed and implemented by JMJ, NM and DM. The ion source was developed by DM, NM and MS. The Be^+ experimental protocols and analysis were conceived and executed by JMJ, NM, DM, JP and GS. The manuscript was written by NM with assistance from DM, JMJ and JP. The manuscript was then edited and improved by the entire collaboration.

 Correspondence and requests for materials should be addressed to NM and DM (Niels.Madsen@cern.ch , daniel.maxwell87@gmail.com).

Data availability statement The datasets generated during and/or analysed during the current study are available from NM and JSH (niels.madsen@cern.ch, jeffrey.hangst@cern.ch) on reasonable request.

Competing financial interests The authors declare no competing financial interests.

Methods / Supplementary Material:

Plasma parameter control and measurement

Positrons are accumulated from a radioactive source based beam using a Surko-type three stage accumulator, where a buffer gas provides the cooling[36]. Subsequently, they are transferred ballistically to the main apparatus through a magnetic beamline, where they are captured using a fast switching gate electrode. The transfer efficiency was around 16% in these experiments, and the number of positrons captured typically fluctuates by more than 10%. To reduce these fluctuations to below 1% we used a combination of a Strong Drive Regime Rotating Wall (SDR) and evaporative cooling (EVC) that we have developed previously[23].

Beryllium is loaded in a similar fashion in the opposite end of the apparatus (Figure 6). Be^+ ions are emitted directly from our ablation target[20] located on the axis of the setup (Figure 1) and subsequently, after they have had time to arrive in the main trap system, dynamically captured using the gate electrode. The mean energy of the Be^+ from ablation is around 20 eV for our ablation laser fluence of 3 Jcm^{-2}. A single capture results in 10^5-10^6 ions. To better control the number of ions we capture multiple batches by repeating the above process several times. The previously captured Be^+ ions are laser cooled with a fixed detuning of -129Γ between batches by moving them to the centre of the trap system (c.f. Figure 6). The large detuning reflects the large energy spread of the captured ions (~20 eV). The number of ions captured in this way fluctuates about 30% between identical runs.

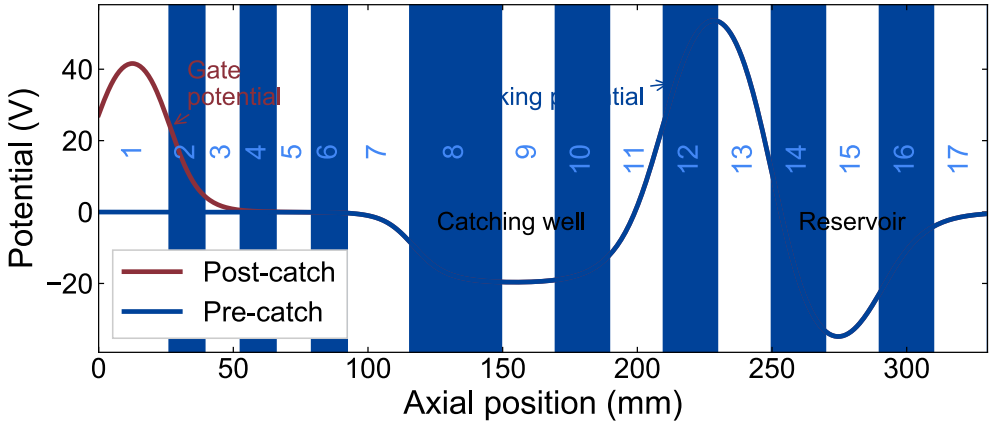

Figure 6 Potentials on axis for Be+ capture and stacking. Shaded and numbered regions represent electrode positions. Ions enter from the left into the blue potential. Subsequently the gate electrode (E1) is raised to 40 V (red potential) to capture them. Ions are then moved to the reservoir where they are combined with previous loads and laser-cooled until the desired number of stacks have been accumulated.

The radial size of the plasmas is controlled by the application of strong-drive regime rotating wall (RW) where a rotating dipolar electric field exerts a torque on the plasma causing it to rotate faster or slower, and thereby compress or expand[37]. In our setup we have two locations where we have the azimuthally split electrodes allowing this, one in the antiproton capture section and one in the positron capture section as indicated on Figure 1. The principle of the RW requires there to be a slight slip between the rotating electric dipole field and the plasmas self-rotation to transfer torque. This slip results in heating of the plasma, and the RW can therefore only be applied effectively for a short while without cooling. Positrons cool through the emission of cyclotron radiation in our 1-3 Tesla fields, but for Be^+ ions we need laser-cooling. As the laser only overlaps in the central part of the apparatus we implemented an arrested procedure where we move the Be^+ plasma between a laser-cooling region, where it is cooled with a fixed detuning at -129Γ, and a RW region multiple times until the desired radial extent is achieved.

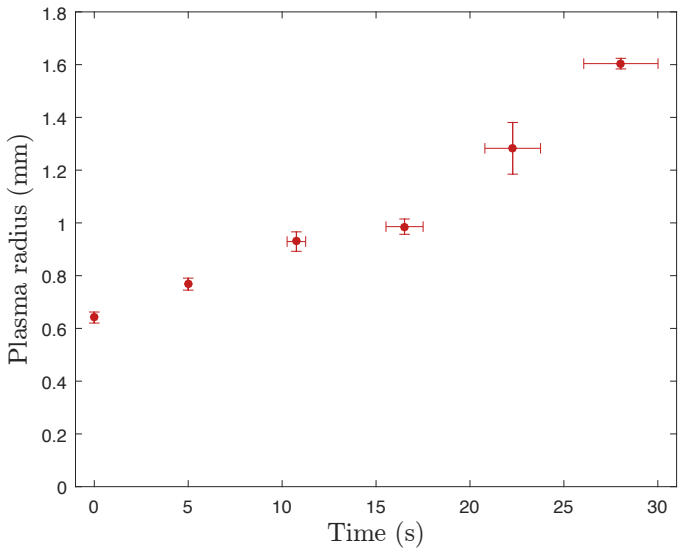

Figure 7 Evolution of the radius of the positron plasma as a function of time during the laser cooling frequency sweep for a mixture of 2.6x10⁶ e⁺ and approximately 4-5x10⁵ Be⁺ ions. Time zero is when the frequency sweep begins. The total sweep time we use to sympathetically cool the positrons to their lowest temperatures is 40 s. It is not possible to measure plasma radii greater than around 1.6 mm with our current MCP imaging diagnostic.

Figure 7 shows measurements of the radial size of the positrons in a mixed plasma during laser-cooling. As discussed in the paper, the mixed plasma also expands during cooling. As shown in Figure 8 this expansion is not observed when only e^+ are present, but it is also present for a pure Be^+-only sample. The total time needed for cooling is therefore an important factor in determining the final radial extent of the positron plasma and therefore its density.

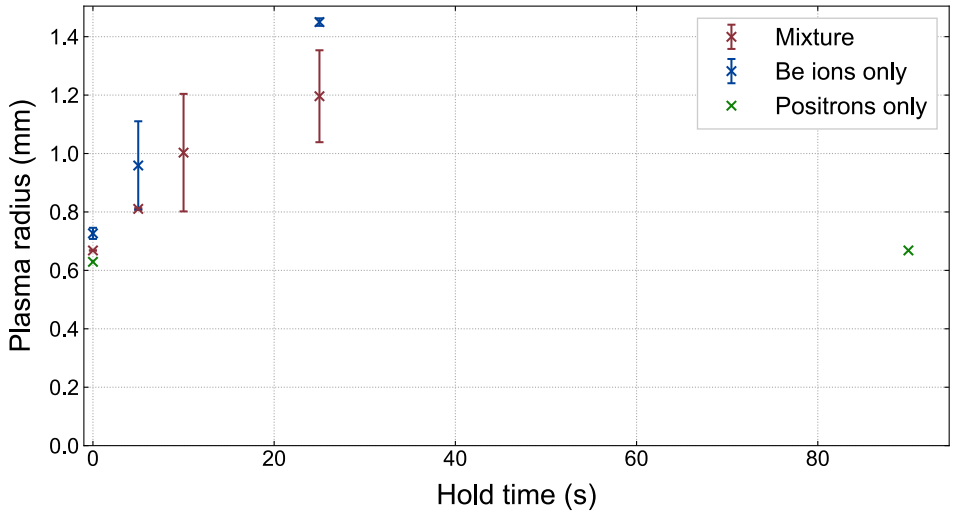

Figure 8 Evolution of the radius of three different plasmas as a function of time without laser-cooling in a 1T field. The mixture (red) consists of 2.6x10⁶ e⁺ and 4x10⁵ Be⁺. The Be⁺ only plasmas contained 4x10⁵ Be⁺. The positrons only plasma contained 2.6x10⁶ e⁺.

As the ion to positron ratio is important for the sympathetic cooling, and only the positron number is stable, we implemented a technique whereby we could measure both the positron temperature and the Be^+ number in each run (except for the special runs where we image the Be^+ plasma to measure the centrifugal separation, as explained in the main part of paper). When measuring axial temperatures by slowly ejecting particles from a well the

temperature information is in the initial exponential tail of particles being ejected[27]. There is thus no reason to eject all the e^+ to measure the temperature. Since Be^+ is centrifugally separated from the e^+ and the potential is the lowest in the center, Be^+ will not be ejected if the well depth is only reduced slightly below the threshold of the first particles escaping. We therefore perform the temperature measurement using a partial ejection by reducing the well to about 60% of the potential where particles first appear (recall, that the e^+ number is reproducible to 1%). Subsequently we close the well and eject the remaining positrons using a 100 ns opening of the well, which is too short for any Be^+ to escape. Finally, we eject the Be^+ ions to the MCP for counting (at this point any original radial extent information will be lost).

Laser setup for ablation and cooling

Two separate laser systems were used for these experiments. Both were located in a laser laboratory adjacent to the main experimental setup. Figure 9 shows a schematic of the setup of the two laser systems. We used a pulsed Nd:YAG laser (Quantel Ultra 20) operating on the 3rd harmonic at 355 nm delivering 6.3 ns long pulses with ~75 µJ per pulse. The pulses are focussed with a f=25 cm convex lens, resulting in a fluence of ~3 Jcm^{-2} on the beryllium metal target to generate Be^+ ions via laser ablation. The ion source is aligned with the beam axis of the main apparatus using a linear translator (c.f. Figure 1). The Toptica TA FHG-PRO system generates 313 nm light for laser cooling by twice doubling the light from a 1252 nm amplified laser diode. A fraction of the 626 nm light from the first doubling stage is sent to a HighFinesse WS8-2 wavemeter for locking the laser frequency. The 313 nm light is circularly polarized with a quarter-wave plate before entering the apparatus.

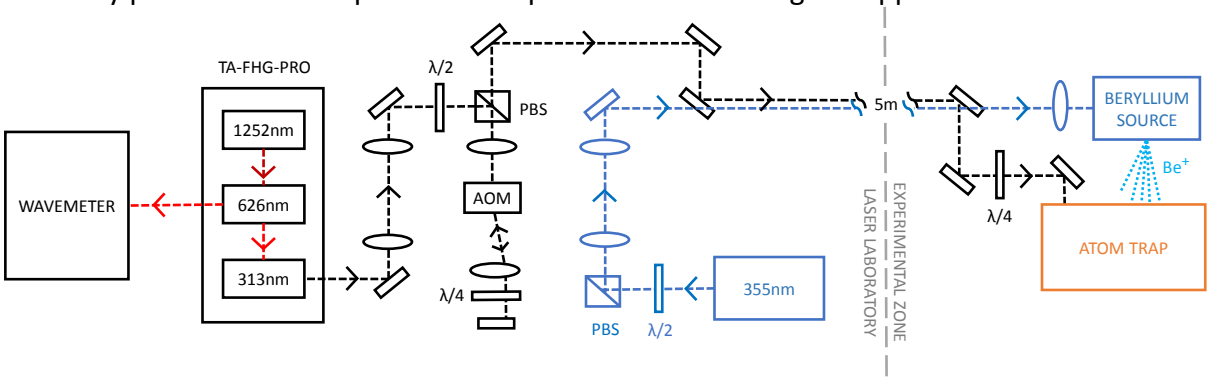

Figure 9 Laser-setup for ablation (blue) and laser-cooling (black). The TA-FHG PRO from Toptica generates 313 nm by two doubling stages of a 1252 nm amplified diode laser. The second harmonic light at 626 nm is sent to a wavemeter for frequency control (see below). The double-pass AOM setup is used to sweep the laser for fluorescence-based detection (the detection geometry was indicated in Figure 1). The polarisation beam splitters (PBS) for both lasers serve, through changes of polarisation to control the power delivered to the experiment. Both lasers are passed through a periscope setup from the laser-room to the experiment. The quarter-wave plate on the 313 nm path before it enters the Atom Trap serves to tune the polarization.

Fluorescence detection

As mentioned in the article the solid angle for observing fluorescing ions is currently limited to about 10^{-6} Sr. In order to measure a Be^+ temperature we can use the AOM (see Figure 9) to chirp the laser-light across the resonance and measure the Doppler-broadened linewidth and thereby the temperature. The AOM has a sweep range of 0-80 MHz (~4Γ). Taken together this allows us only to measure the temperature of Be^+ samples colder than ~500 mK. Figure 10 shows an example of a measurement of ~1M Be^+ ions laser-cooled with a final

detuning of -3Γ. To extract the Be^+ temperature we fit the left hand side of the fluorescence peak with a Voigt function. The asymmetry resulting from heating of the ions when the laser is on the high frequency side of the resonance means that the right hand side of the peak is ignored in the analysis. In order to extract a temperature the Voigt function is deconvolved into its Lorentzian and Gaussian components. From the Gaussian full width at half maximum the ion temperature can then be calculated. Due to limitations in the AOM frequency range and the small solid angle we cannot currently conduct fluorescence based temperature diagnostics of Be^+ in mixed samples of Be^+ and e^+ where the Be^+ number is much lower and the temperature higher than in the example measurement in Figure 10.

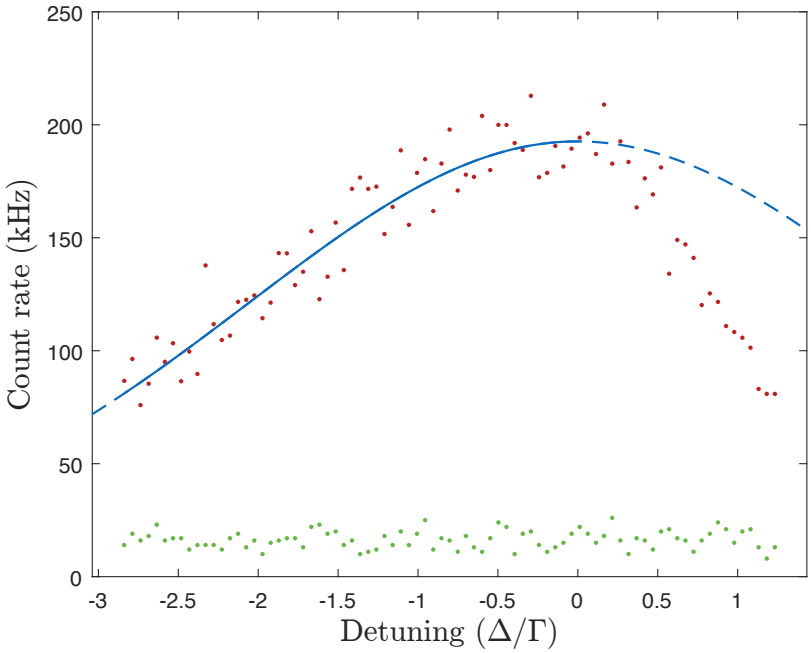

Figure 10 Fluorescence signal from a pure Be^+ plasma as the frequency of the cooling laser is scanned across the laser cooling transition. The background corrected signal (red points) has been fit with a Voigt function (blue solid line) on the left-hand side of the peak. It is clear that the function fits poorly if it is continued onto the right-hand side of the peak (blue dashed line) where the fluorescence signal drops off rapidly. This sharp decay in signal is attributed to heating of the ions when the laser detuning is on the blue side of the resonance. The Voigt profile corresponds to an ion temperature of approximately 150 mK. The background signal on the detector when no ions are loaded, which comes mainly from scatter of the laser beam within the apparatus, is shown for reference (green points).

Be^+ laser frequency control

The frequency of the 313 nm cooling laser is regulated via modulation of the master laser diode current in a PID loop. The modulation signal is provided by a wavemeter which is continuously measuring the frequency of the second harmonic (at 626 nm) of the master laser. The wavemeter is calibrated at the beginning of every experimental run using a stable He-Ne laser as a frequency reference. When sweeping the frequency to laser cool the Be^+ ions, and sympathetically cool positrons, we discretely step the frequency setpoint such that the laser frequency changes at an average rate of approximately 70 MHz/s between setpoints. Discrete steps in the setpoint were used to ensure that the PID loop changed the frequency of the laser smoothly, and slowly enough such that the ions are continuously cooled from their initial high temperature. Unfortunately, due to hardware resources shared with other aspects of the ALPHA apparatus, the wavemeter was not fully integrated with the control system managing sympathetic cooling, which resulted in latency and jitter

when requesting changes to the laser frequency. The relatively large horizontal error bars in Figure 7 are a result of this jitter. Another consequence of this uncertainty is that we could not use this method of frequency modulation when measuring fluorescence spectra. Faster, deterministic frequency sweeps were performed when measuring the Doppler broadened fluorescence spectra of the Be^+ ions. In this case we used an AOM to sweep the frequency of the light by 80 MHz in 80 ms (Figure 9). By performing several fluorescence measurements over different days, we have determined that the location of the laser-cooling resonance is consistent to within 9 MHz (standard deviation), corresponding to ~Γ/2. The apparent fluctuation in the resonance location is most likely due to a combination of the imperfect laser frequency lock, the calibration and precision of the wavemeter, and our ability to locate the resonance of the strongly asymmetric line shape.

[1] C. D. Anderson, The Positive Electron, Phys. Rev. **43**, 491 (1933)
[2] P. A. M. Dirac, A theory of electrons and protons, Proc. Roy. Soc. A **126**, 360 (1930)
[3] F. Tuomisto and I. Makkonen, Defect identification in semiconductors with positron annihilation: Experiment and theory, Rev. Mod. Phys. **85**, 1583 (2013)
[4] C. Hugenschmidt, Positrons in surface physics, Surf. Sci. Rep. **71**, 547 (2016)
[5] D. L. Bailey, *et al.*, Positron Emission Tomography, (Springer London Ltd), ISBN 978-1-85233-798-8, (2005)
[6] M. Deutsch, Evidence for the Formation of Positronium in Gases, Phys. Rev. **82**, 455 (1951)
[7] S. G. Karshenboim, Precision physics of simple atoms: QED tests, nuclear structure and fundamental constants, Phys. Rep. **422**, 1 (2005)
[8] G. Baur, *et al.*, Production of Antihydrogen, Phys. Lett. B **368**, 251 (1996)
[9] M. Amoretti, *et al.*, Production and detection of cold antihydrogen atoms, Nature **419**, 456 (2002)
[10] C. H. Storry, *et al.*, First laser-controlled antihydrogen production, Phys. Rev. Lett. **93**, 263401 (2004)
[11] V. A. Kostelecky and A. J. Vargas, Lorentz and CPT tests with hydrogen, antihydrogen and related systems, Phys. Rev. D **92**, 056002 (2015)
[12] M. Ahmadi, *et al.* Characterization of the 1S-2S transition in antihydrogen, Nature **557**, 71 (2018)
[13] M. Ahmadi, *et al.*, Antihydrogen accumulation for fundamental symmetry tests, Nat. Comm. **8**, 681 (2017)
[14] S. Jonsell and M. Charlton, On the formation of trappable antihydrogen, N. J. Phys. **20**, 043049 (2018)
[15] N. Madsen, *et al.*, Spatial Distribution of Cold Antihydrogen Formation, Phys. Rev. Lett. **94**, 033403 (2005)
[16] L. Schmöger, *et al.*, Coulomb crystallization of highly charged ions, Science **347**, 1233 (2015)
[17] M. D. Barrett *et al.*, Sympathetic cooling of $^9Be^+$ and $^{24}Mg^+$ for quantum logic, Phys. Rev. A **68**, 042302 (2003)
[18] B. M. Jelenkovic *et al.*, Sympathetically cooled and compressed positron plasma, Phys. Rev. A **67**, 063406 (2003)
[19] N. Madsen, F. Robicheaux and S. Jonsell, Antihydrogen trapping assisted by sympathetically cooled positrons, New. J. Phys. **16**, 063046 (2014)
[20] M. Sameed, D. Maxwell and N. Madsen, Ion generation and loading of a Penning trap using pulsed laser ablation, New J. Phys. **22**, 013009 (2020)
[21] C. Amole, *et al.*, In situ electromagnetic field diagnostics with an electron plasma in a Penning-Malmberg trap, New. J. Phys. **16**, 013037 (2014)
[22] C. Amole *et al.*, The ALPHA antihydrogen trapping apparatus, Nucl. Instr. and Meth. A **735**, 319 (2014)
[23] M. Ahmadi, *et al.* Enhanced Control and Reproducibility of Non-Neutral Plasmas, Phys. Rev. Lett. **120**, 025001 (2018)
[24] X. P. Huang,*et al.*, Steady-State Confinement of Non-neutral Plasmas by Rotating Electric Fields, Phys. Rev. Lett. **78**, 875 (1997)
[25] G.B. Andresen, *et al.* Compression of Antiproton Clouds for Antihydrogen Trapping, Phys. Rev. Lett. **100**, 203401 (2008)
[26] G.B. Andresen, *et al.*, Antiproton, positron and electron imaging with a microchannel plate/phosphor detector, Rev. Sci. Inst. **80**, 123701 (2009)
[27] D. L. Eggelston, *et al.*, Parallel energy analyzer for pure electron plasma devices, Phys. Fluids B: Plas. Phys. **4**, 3432 (1992)
[28] G. B. Andresen, *et al.*, Evaporative cooling of antiprotons to cryogenic temperatures, Phys. Rev. Lett. **105**, 013003 (2010)

[29] E.D. Hunter *et al.*, Plasma temperature measurement with a silicon photomultiplier (SiPM), Rev. Sci. Inst. **91**, 103502 (2020)
[30] D. H. E. Dubin and T.M. O'Neil, Trapped nonneutral plasmas, liquids, and crystals (the thermal equilibrium states), Rev. Mod. Phys. **17**, 87 (1999)
[31] T. M. O'Neil, Centrifugal separation of a multispecies pure ion plasma, Phys. Fluids **24**, 1447 (1981)
[32] A.A. Kabantsev, J.H. Yu, R.B. Lynch and C.F. Driscoll, Trapped particles and asymmetry-induced transport, Phys. Plas. **10**, 1628 (2003)
[33] G.B. Andresen *et al.*, Centrifugal separation and equilibration dynamics in an electron-antiproton plasma, Phys. Rev. Lett. **106**, 145001 (2011)
[34] J. Fajans *et al.*, Effects of Extreme Magnetic Quadrupole Fields on Penning Traps and the Consequences for Antihydrogen Trapping, Phys. Rev. Lett. **95**, 155001 (2005)
[35] E. Butler, PhD Thesis, Antihydrogen Formation, Dynamics and Trapping, Sec 3.5, Swansea University (2011)
[36] T.J. Murphy and C.M. Surko, Positron trapping in an electrostatic well by inelastic collisions with nitrogen molecures, Phys. Rev. A **46**, 5695 (1992)
[37] J. R. Danielson and C.M. Surko, Torque-Balanced High-Density Steady States of Single-Component Plasmas, Phys. Rev. Lett. **94**, 035001 (2005)